

## Growth and characterization of Ga-doped ZnO thin films deposited by sol-gel dip-coating method

Sang-heon Lee<sup>1</sup>, Wonshoup So<sup>1</sup>, Jae Hak Jung<sup>1\*</sup>, Min Su Kim<sup>2</sup>, Soaram Kim<sup>2</sup> and Jae-Young Leem<sup>2\*</sup>

<sup>1</sup>*School of Chemical Engineering, Yeungnam University, Gyeongsan 712-749, Republic of Korea*

<sup>2</sup>*Department of Nano Systems Engineering, Center for Nano Manufacturing, Inje University, Gimhae 621-749, Republic of Korea*

<sup>1\*</sup>E-mail: jhjung@ynu.ac.kr, <sup>2\*</sup>E-mail: jyleem@inje.ac.kr

### I. INTRODUCTION

Zinc oxide (ZnO) is an essential starting material for the construction of nanoscale structures because of its low cost and favorable electrical, optoelectronic, and luminescent properties. ZnO has a wide direct band gap of 3.37 eV at room temperature (RT) [1], and its exciton binding energy is relatively large at a value of 60 meV, which ensures efficient excitonic emission up to RT [2].

Compared to undoped ZnO, impurity-doped ZnO displays lower resistivity and higher stability. ZnO has been doped with Al, Ga, In, B, Si, Ge, Ti, Zr, Hf, and F [3-7]. Among the metal dopants used, Ga doping seems to be the most successful and promising approach because of advantages such as the comparable ionic and covalent radii of Ga and ZnO (Ga: 0.62 and 1.26 Å, ZnO: 0.74 and 1.34 Å), resulting in relatively small ZnO lattice deformations, even at high Ga concentrations. Moreover, Ga is less reactive and more resistant to oxidation than Al. The sol-gel process is especially attractive because it is easily performed in the laboratory for the synthesis of semiconducting thin films of controlled thickness and overall dimensions. In addition, the process is of low cost and could thus find many technological applications.

### II. EXPERIMENTAL PROCEDURE

The precursors used to prepare the films were zinc acetate dihydrate, 2-methoxyethanol, and monoethanolamine (MEA) as the sol-stabilizer. Zinc acetate was added to 2-methoxyethanol to obtain a concentration of 0.3 M. Ga dopant was added in the form of GaCl<sub>3</sub> with varying Ga/Zn ratio of from 0 to 5 at.%. The solutions were then used to prepare thin films on quartz substrates by drain coating at withdrawal rates of 8 cm/min. After each dip coating, the films were incubated in air in an oven at 150 °C for 10 min. This process was repeated 5 times for each sample. The samples were finally heated at 500 °C for 60 min. Scanning electron microscopy (SEM), X-ray diffraction (XRD), photoluminescence (PL), and UV-visible spectroscopy were carried out to investigate the effect of the Ga concentration on the structural and optical properties of the GZO thin films.

### III. RESULTS AND DISCUSSION

Figure 1 shows the SEM images of the GZO thin films with different Ga concentrations: (a) 0, (b) 1, (c) 3, and (d) 5 at.%. The ZnO and GZO thin films exhibited rough surfaces with a particle-like structure. The particle-like and porous structure was particularly evident in the sol-gel synthesized ZnO thin films. With an increase in the Ga concentration, the particle size slightly decreased. In the case of Al-doped ZnO thin films (AZO), it was found that the surface morphology was strongly dependent on the Al concentration [8]. Interestingly, with an increase in Al concentration, the morphology of the AZO thin films changed to nanorod-like structures. In the case of the GZO thin films, no significant change in morphology was observed, which might be due to the comparable ionic and covalent radii of Ga and ZnO, as mentioned above.

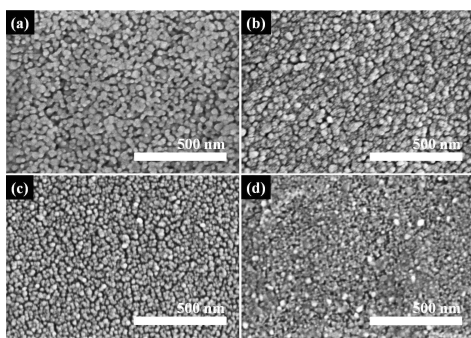


Fig. 1. SEM images of the GZO thin films with different Ga concentrations: (a) 0, (b) 1, (c) 3, and (d) 5 at.%.

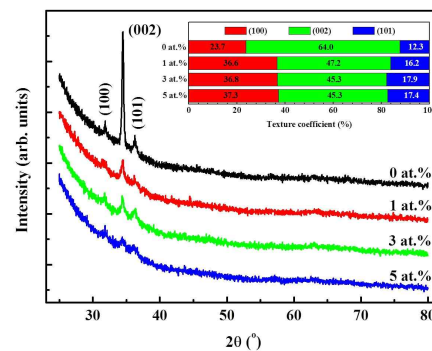


Fig. 2. XRD patterns of the GZO thin films with different Ga concentrations: (a) 0, (b) 1, (c) 3, and (d) 5 at.%. The inset shows the texture coefficient of the GZO thin films with different Ga concentrations: (a) 0, (b) 1, (c) 3, and (d) 5 at.%.

Figure 2 shows the XRD patterns of the GZO thin films with different Ga concentrations: (a) 0, (b) 1, (c) 3, and (d) 5 at.%. For all GZO thin films, three ZnO diffraction peaks were observed at 31°, 34°, and 36° corresponding to ZnO (100), (002), and (101) planes, respectively. It is well known that ZnO grows in *c*-axis preferred orientation under normal growth conditions because the (001) basal plane in ZnO possesses the lowest surface energy, leading to a preferred growth in the [001] direction. With increasing Ga concentrations, the intensity of the ZnO (001) diffraction peak decreased dramatically. To describe the preferred orientation, the texture coefficient ( $TC_{(hkl)}$ ) was calculated using the following equation [9]:

$$TC_{(hkl)} = \frac{I_{(hkl)} / I_{0(hkl)}}{1 / N \sum_N I_{(hkl)} / I_{0(hkl)}}, \quad (1)$$

where  $N$  is the number of diffraction peaks, and  $I_{(hkl)}$  and  $I_{0(hkl)}$  are the integrated intensities of the  $(hkl)$  reflection of GZO thin films containing the textured and randomly oriented crystallites. It is clear from this definition that a deviation of  $TC$  from unity implies the growth of GZO thin films in a preferred orientation along the particular diffraction plane. As

shown in the inset of Figure 2, the value of  $TC_{(002)}$  of the GZO thin films decreased with Ga doping, although the change was not particularly large.

Figure 3 shows the optical transmittance of the GZO thin films with different Ga concentrations: (a) 0, (b) 1, (c) 3, and (d) 5 at.%. The absorption edge was observed at 360 nm with a transparency of over 80% in the visible range. The optical transmittance in the UV range decreased with increasing Ga concentration. The calculated absorption coefficient  $\alpha(\lambda)$  of the GZO thin films is depicted in the inset of Figure 3. The  $\alpha(\lambda)$  of ZnO-based materials can be calculated by [10]:

$$T = \exp[-\alpha(\lambda)d], \quad (2)$$

where  $T$  is the optical transmittance and  $d$  is the thickness of the GZO thin films. The  $\alpha(\lambda)$  of materials with a direct band gap is larger than 100 - 1000 times that of materials with an indirect band gap. The fundamental absorption edge of the GZO thin films results from electron transitions from the valence band into the conduction band and, therefore, this edge can be used to calculate the optical band gap of the ZnO thin films. The  $\alpha(\lambda)$  in the UV range of the GZO thin films decreased with Ga doping.

The incorporation of impurities into semiconductors often results in the formation of band in the band gap. The  $\alpha(\lambda)$  near the fundamental absorption edge exhibits an exponential dependency on the incident photon energy and obeys the empirical Urbach relation, in which  $\ln\alpha$  varies as a function of  $h\nu$ . The Urbach energy  $E_U$  can be calculated by the following relation [11]:

$$\alpha = \alpha_0 \exp\left(\frac{h\nu}{E_U}\right), \quad (3)$$

where  $\alpha_0$  is a constant.  $E_U$  refers to the width of the exponential absorption edge. Figure 4 shows the variation of  $\ln\alpha$  vs photon energy for the GZO thin films with different Ga concentrations: (a) 0, (b) 1, (c) 3, and (d) 5 at.%. As shown in the inset of Figure 4, the  $E_U$  value of the GZO thin films gradually increased from 84.2 to 153.0 meV with an increase in the Ga concentration. Apparently, the concentration of Ga determines the width of the localized states in the optical band of the GZO thin films.

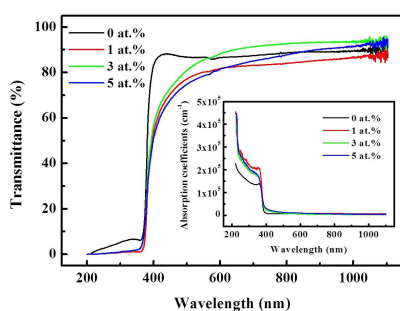


Fig. 3

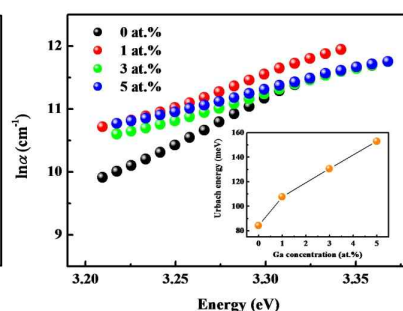


Fig. 4

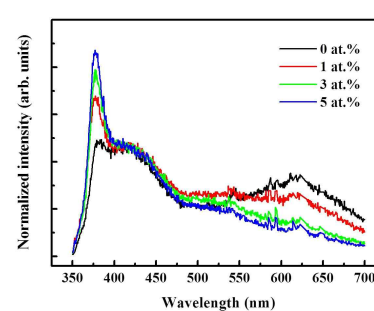


Fig. 5

Fig. 3. Optical transmittance of the GZO thin films with different Ga concentrations

Fig. 4. The variation of  $\ln\alpha$  with photon energy for the GZO thin films with different Ga concentrations

Fig. 5. Normalized PL spectra of the GZO thin films with different Ga concentrations

Figure 5 shows the normalized PL spectra of the GZO thin films with different Ga concentrations: (a) 0, (b) 1, (c) 3, and (d) 5 at.%. For the pure ZnO thin films (0 at.%), three emission peaks were observed at 380, 419, and 621 nm. Here, the peak at 380 nm is a near-band-edge emission (NBE) peak generated by exciton recombination. The other two peaks, at 419 and 621 nm, are deep-level emission (DLE) peaks caused by structural defects in the ZnO thin films, i.e., oxygen vacancies ( $V_O$ ) and zinc interstitials ( $Zn_i$ ) for the 419 nm peak [12], and excess oxygen for the 621 nm peak. The intensity of the NBE peak increased with increasing Ga concentration because of an increase in the electron carrier concentration. It was furthermore noted that the intensity of the peak at 621 nm decreased gradually with increasing Ga concentration, which possibly resulted from a decrease in the excess oxygen atoms in the GZO thin films. It should be noted that the Ga-O bond is stronger than that of Zn-O. By Ga incorporation, the number of excess oxygen atoms that exist in the GZO thin films could therefore be decreased, leading to a decreased intensity of the 621 nm peak.

#### IV. CONCLUSIONS

The structural and optical properties of the GZO thin films deposited by a sol-gel dip-coating method and incorporating different Ga concentrations were investigated. The GZO thin films exhibited a rough surface with a particle-like structure. With increasing Ga concentration, the particle size slightly decreased without affecting the surface morphology. The optical transmittance in the visible region of the GZO thin films was above 80%. In addition, three emission peaks were observed in the UV and visible region of the ZnO thin films. With increasing Ga concentration, the intensity of the UV emission peak increased, while that of the red emission peak decreased.

#### REFERENCES

1. D. M. Bagnall, Y. F. Chen, Z. Zhu, T. Yao, S. Koyama, M. Shen and T. Goto, *Appl. Phys. Lett.* **70**, 2230 (1997).
2. D. C. Look, *Mater. Sci. Eng. B* **80**, 381 (2001).
3. T. Minami, H. Nanto and S. Takata, *Jpn. J. Appl. Phys.* **23**, L280 (1984).
4. B. H. Choi, H. B. Im, J. S. Song and K. H. Yoon, *Thin Solid Films* **193**, 712 (1990).
5. B. J. Lokh, P. S. Patil and M. D. Uplane, *Physica B* **302-303**, 59 (2001).
6. T. Minami, H. Sato, N. Nanto and S. Takata, *Jpn. J. Appl. Phys.* **25**, L776 (1986).
7. J. Hu and R. G. Gordon, *Sol. Cells* **30**, 437 (1991).
8. N. Huang, C. Sun, M. Zhu, B. Zhang, J. Gong and X. Jiang, *Nanotechnology* **22**, 265612 (2011).
9. M. Benhaliliba, C. E. Benouis, M. S. Aida, F. Yakuphanoglu and A. S. Juarez, *J. Sol-Gel Sci. Technol.* **55**, 335 (2010).
10. K. H. Kim, K. C. Park and D. Y. Ma, *J. Appl. Phys.* **81**, 7764 (1997).
11. F. Urbach, *Phys. Rev.* **92**, 1324 (1953).
12. K. Shin, K. Prabakar, W. P. Tai, J. H. Oh, C. Lee, D. W. Park and W. S. Ahn, *J. Korean Phys. Soc.* **45**, 1288 (2004).